Journal Pre-proof

Structure, infrared reflectivity spectra and microwave dielectric properties of a low-firing microwave dielectric ceramic $Pr_2Zr_3(MoO_4)_9$

Jinjie Zheng, Chunfang Xing, Yaokang Yang, Shuaixia Li, Haitao Wu, Zhihao Wang

PII: S0925-8388(20)30256-5

DOI: https://doi.org/10.1016/j.jallcom.2020.153893

Reference: JALCOM 153893

To appear in: *Journal of Alloys and Compounds*

Received Date: 23 July 2019

Revised Date: 16 December 2019

Accepted Date: 16 January 2020

Please cite this article as: J. Zheng, C. Xing, Y. Yang, S. Li, H. Wu, Z. Wang, Structure, infrared reflectivity spectra and microwave dielectric properties of a low-firing microwave dielectric ceramic $Pr_2Zr_3(MoO_4)_9$, *Journal of Alloys and Compounds* (2020), doi: https://doi.org/10.1016/j.jallcom.2020.153893.

Author Contribution Statement

Jinjie Zheng: Methodology, Investigation, Data curation, Writing-Original draft

Chunfang Xing: Writing- Reviewing and Editing

Yaokang Yang: Software, Validation

Shuaixia Li: Investigation

Haitao Wu and Zhihao Wang: Supervision, Resources, Project administration, Funding acquisition

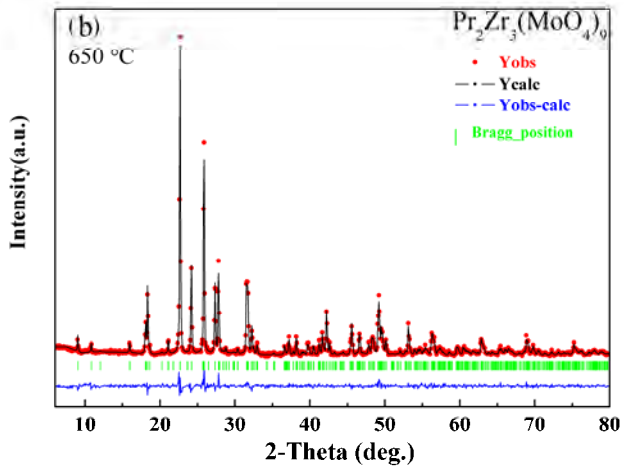
(b)
650 °C
$Pr_2Zr_3(MoO_4)_9$
Yobs
Ycalc
Yobs-calc
Bragg_position
Intensity(a.u.)
2-Theta (deg.)
10
20
30
40
50
60
70
80

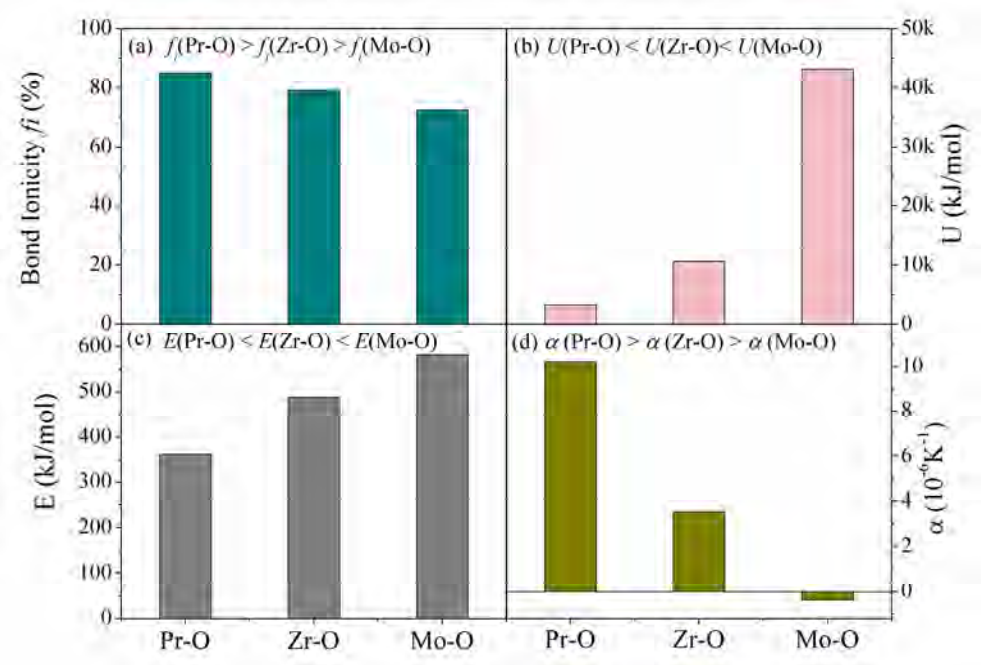
(a) f_i(Pr-O) > f_i(Zr-O) > f_i(Mo-O)
(b) U(Pr-O) < U(Zr-O) < U(Mo-O)
(c) E(Pr-O) < E(Zr-O) < E(Mo-O)
(d) α (Pr-O) > α (Zr-O) > α (Mo-O)
Bond Ionicity f_i (%)
U (kJ/mol)
E (kJ/mol)
α ($10^{-6}K^{-1}$)
Pr-O
Zr-O
Mo-O

Structure, infrared reflectivity spectra and microwave dielectric properties of a low-firing microwave dielectric ceramic $Pr_2Zr_3(MoO_4)_9$

Jinjie Zheng[a], Chunfang Xing[a], Yaokang Yang[a], Shuaixia Li[a], Haitao Wu[a,*], Zhihao Wang[b,*]

[a]School of Materials Science and Engineering, University of Jinan, Jinan, 250022, PR China

[b]School of Materials Science and Engineering, Qilu University of Technology (Shandong Academy of Sciences), Jinan, 250353, PR China

Abstract

$Pr_2Zr_3(MoO_4)_9$ ceramics were prepared by solid state reaction method and the microwave dielectric properties were investigated for the first time. Single-phase $Pr_2Zr_3(MoO_4)_9$ ceramics with a space group R-3c were obtained in the whole sintering temperature range (600-800 °C) confirmed by X-ray diffraction (XRD) and Rietveld refinement. SEM images combined with high relative density (95.7 %) suggested that well-densed $Pr_2Zr_3(MoO_4)_9$ ceramic could formed at low sintering temperature 650 °C. The intrinsic factors affecting dielectric properties were analyzed according to chemical bonds theory of complex crystals and infrared spectra. Typically, the novel microwave dielectric ceramic $Pr_2Zr_3(MoO_4)_9$ sintered at 650 °C exhibited desirable dielectric properties combination: ε_r = 10.72, $Q{\cdot}f$ = 64,200GHz (at 9.6 GHz) and τ_f = -13.0 ppm/°C.

Keywords: Chemical bonds theory of complex crystals, $Pr_2Zr_3(MoO_4)_9$, Microwave dielectric ceramic, Infrared spectra

1. Introduction

As the Tactile Internet (5th generation wireless systems) comes from nowhere, microwave dielectric materials are now facing ever greater attention [1,2]. In order to meet the applications of dielectric resonator, microwave ceramics are required to possess low sintering temperature, suitable permittivity (ε_r) for integration, high quality factor ($Q{\cdot}f$) to ensure excellent frequency selection and a near zero temperature coefficient of resonant frequency (τ_f) to guarantee high thermal stability [3,4]. So there is a need to search for novel materials that meet the above requirements. Furthermore, the relationships between internal crystal structure and dielectric properties are also need to be investigated [2].

For the moment, there are more desirable findings in the research on microwave dielectric ceramics, including studies on lowering sintering temperature and low-temperature co-fired ceramic (LTCC) applications [6-9], ion-doping and optimizing phase composition for low dielectric loss [10-13], improving temperature stability by the preparation of composite ceramics [14-15], the use of cold sintering method [16], and exploration

* Corresponding author.
Tel.: +86 531 82769782; fax: +86 531 87974453.
E-mail address: mse_wuht@ujn.edu.cn (H.T. Wu).

of novel ceramic systems with high performance [17-21]. What's more, some analytical methods such as Raman spectroscopy and neutron diffraction are widely used in the field of dielectric materials to analyze crystal structures [22-26]. Notably some molybdate compounds have been reported successively as microwave dielectric materials due to their lower sintering temperature and adjustable dielectric properties [27,28]. Zhou et al. reported a series of $XMoO_4$ ceramics sintered at less than 900 °C with a tetragonal scheelite structure, such as $[Ca_{0.55}(Sm_{1-x}Bi_x)_{0.3}]MoO_4$ [27] and $(Ca,Bi)(Mo,V)O_4$ [28] etc. These $XMoO_4$ compounds exhibited ε_r in the range of 10~35 and 10,000~70,000 GHz for $Q{\cdot}f$. This inspired us to look for other Mo-based materials.

Double molybdates of rare earth elements and zirconium $Ln_2(MoO_4)_3$-$Zr(MoO_4)_2$ have been extensively studied because of their scientific and technological importance. The structural, luminescent and thermal characteristics of $Ln_2Zr_3(MoO_4)_9$ (Ln = Ce, Pr, Eu) have been reported by Dorzhieva et al [29]. Bazarova et al. constructed the phase diagrams of $Ln_2(MoO_4)_3$-$Zr(MoO_4)_2$ double molybdates systems and studied the dielectric characteristics of $Pr_2Zr_3(MoO_4)_9$ ceramics at frequencies of 0.1-200 kHz [30]. What's more, the microwave dielectric properties of a series of $Ln_2Zr_3(MoO_4)_9$ (Ln = La, Nd, Sm, Eu, and Gd) ceramics have been reported [31-35]. $La_2Zr_3(MoO_4)_9$ ceramics with a ε_r of 10.8, $Q{\cdot}f$ =50,628GHz (at 9 GHz) and τ_f = -38.8 ppm/°C were firstly reported by Liu et al [31]. Zhang et al. improved the quality factor values of the $La_2Zr_3(MoO_4)_9$ matrix to 80,658 GHz by Ti^{4+}-doping, and they also studied the relationship between the chemical bond characteristics and microwave dielectric properties of $La_2(Zr_{1-x}Ti_x)_3(MoO_4)_9$ ceramics [32]. Besides, $Nd_2Zr_3(MoO_4)_9$, $Sm_2Zr_3(MoO_4)_9$, $Eu_2Zr_3(MoO_4)_9$ and $Gd_2Zr_3(MoO_4)_9$ ceramics have also been reported [33-35]. All of them belonged to R-3c space group and possessed a low sintering temperature (< 900 °C) as well as a high quality factor (> 40,000 GHz). However, the dielectric properties of the $Pr_2Zr_3(MoO_4)_9$ (PZM) ceramics at microwave frequencies were not investigated until now. Therefore, in search for another dielectric material with low sintering temperature, $Pr_2Zr_3(MoO_4)_9$ (PZM) ceramics were fabricated by solid-state route in this work and the crystal structure, sinterability, and microwave dielectric properties were deeply discussed. Moreover, the intrinsic factors affecting dielectric properties were explored by calculating the chemical bond parameters (iconicity, bond energy, lattice energy, and thermal expansion coefficient) and fitting the phonon parameters.

2. Experimental procedures

PZM ceramics were prepared via solid-state route. Firstly, stoichiometric high-purity oxide powders of Pr_6O_{11}, ZrO_2, and MoO_3 were weighed and ball milled for 24 h in a nylon bottle with alcohol medium. Secondly, these powders were calcined at 750 °C for 6 h and re-milled for 24 h. Thirdly, the resulting mixture were pressed

into cylinders with 10 mm in diameter as well as 6 mm in thickness using 10 wt % paraffin wax as a blinder, and the wax was removed by heating at 500 °C for 4 h. Finally, these green pellets were sintered at 600-800 °C in air for 6 h.

The phase compositions of calcined samples were studied by X-ray diffraction (XRD) technique using a Bruker D8 Advance Diffractometer at the 2θ range of 5-80°. Rietveld refinements using FullProf software were performed to analyze crystal structure. Scanning electron microscope (SEM) (QUANTA FEG250, FEI, America) was carried out to observe the surface morphology. Infrared reflectivity spectrum was measured using a Bruker IFS 66v FT-IR spectrometer at room temperature. Permittivity and quality factors were measured by a vector network analyzer (N5234A, Agilent Co., USA) with Hakki-Coleman dielectric resonator method in $TE_{01\delta}$ mode [36,37]. The τ_f values were calculated with the following equation:

$$\tau_f = \frac{f_2 - f_1}{f_1(T_2 - T_1)} \quad (1)$$

where f_1 and f_2 were the resonant frequency at T_1 (25 °C) and T_2 (85 °C), respectively.

3. Results and discussion

Fig. 1 (a) presented XRD patterns for the PZM ceramics sintered in the temperatures range of 600-800 °C. The diffraction peaks for samples sintered at diverse temperatures were similar and matched with the standard pattern of PZM (ICDD File No. 51-1851), confirming that the synthesis of single-phase PZM. For the purpose of study the crystal structure in detail, Rietveld refinements of the XRD patterns were done by FullProf software based on a structural model of $Nd_2Zr_3(MoO_4)_9$ (ICSD #92600) [38]. The refined plots for PZM samples sintered at 650 °C were shown in Fig. 1 (b). Table 1 listed refined parameters including *a, b, c,* V_{unit}, and reliability factors (R_{wp}, R_p, and χ^2). Notably all the χ^2 values were no more than 2.1, implying the reliability of the refinement.

Schematics crystal structure and single oxygen polyhedron of different central atoms of PZM were shown in Fig. 2 as well. Pr, Zr and Mo coordinated with 9, 6 and 4 oxygen atoms to form polyhedra [PrO_9], [ZrO_6] and [MoO_4], respectively. In three-dimensional lattices, the [MoO_4] hexahedral shared oxygen with the [ZrO_6] octahedron and [PrO_9] tetrakaidecahedron, but there was no shared oxygen between [ZrO_6] and [PrO_9] , that was to say, [MoO_4] served as a bridge between them two. In brief, the structure could be regarded as three kinds of oxygen polyhedra connected by vertices.

The apparent densities as well as relative densities of PZM samples as functions of sintering temperatures were shown in Fig. 3. As the sintering temperature went from 600 to 650 °C, the apparent density increased from 3.56 to 3.88 g/cm^3, meanwhile the theoretical density went up from 87.9 to 95.7. Thereafter, the density curves

remained steady and the values of relative density were not less than 95 % for PZM ceramics sintered at 650-800 °C. Therefore, it can draw a conclusion that PZM ceramics could be well densified at 650 °C.

Fig. 4 exhibited the SEM images of surfaces for PZM ceramics sintered at 600-800 °C for 6 hours. It could be seen pores in Fig. 4 (a) clearly, which accounted for the low density values for PZM sintered at 600 °C in Fig. 3. When samples were sintered at 650-800 °C, dense and uniform grain micrographs with average grain size of about 0.9 μm were obtained as shown in Fig. 4 (b-e). What's more, Energy Dispersive X-ray microanalysis system (EDS) (Fig. 4(f)) was carried on the grain chosen randomly from sample sintered at 650 °C. The atom molar ratio of Pr, Zr, Mo, and O was 1.7 : 3.1 : 8.1 : 36.9, which was roughly consistent with the theoretical composition of $Pr_2Zr_3(MoO_4)_9$.

Fig. 5 presented the dependence of ε_r values for PZM ceramics as the temperature varies. The relative permittivity values went up and then reached a stable value (~11) at 650 °C. In particular, the variations in ε_r values with sintering temperature were just well consistent with that of density, indicating that density played a key role in affecting ε_r values for PZM in the lower temperature range. To eliminate the effect of porosity on permittivity, the porosity corrected values were calculated by Bosman and Having's way as shown in the following equation [39]:

$$\varepsilon_{corr} = \varepsilon_{mea}(1+1.5P) \tag{2}$$

where P was the porosity fraction. As shown in Fig. 5, the ε_{corr} exhibited weak dependence on sintering temperatures and fluctuated at about 11.2, which was so close to the ε_{mea} value (~11) for the ceramics sintered in the temperature range of 650 to 800 °C. Besides density, permittivity was also influenced by intrinsic factors, such as dielectric polarizabilities and iconicity of chemical bond [2,34]. In this work, the theoretical dielectric polarizability (α_{theo}) was calculated by ion additivity rule equation:

$$\alpha_{theo} = 2\alpha(Pr^{3+})+3\alpha(Zr^{4+})+9\alpha(Mo^{6+})+36\alpha(O^{2-}) \tag{3}$$

The ion polarizability of Pr^{3+}(5.32), Zr^{3+}(3.25) and O^{2-}(2.01) were reported by Shannon [40], and ion polarizability of Mo^{6+}(3.28) was suggested by Choi [41]. And observed dielectric polarizability (α_{obs}) could be derived from Clausius-Mosotti equation:

$$\alpha_{obs} = \frac{1}{b}V_m\frac{\varepsilon_{mea}-1}{\varepsilon_{mea}+2} \tag{4}$$

where b, V_m and ε_{mea} are constant value ($4\pi/3$), molar volume and measured permittivity for PZM ceramic, respectively. The calculated results (α_{theo} = 122.27 and α_{obs} = 142.04) were roughly close and the slight difference might be due to measurement errors.

The variation tendencies of $Q{\cdot}f$ and τ_f values of PZM ceramics as functions of sintering temperatures were presented in Fig. 6. Like the dielectric constant, the tendency of quality factor values with temperature was same to density, suggesting that density could be a dominating role in affecting dielectric loss for less dense samples. Notably, the maximum $Q{\cdot}f$ value 64,200 GHz was obtained in PZM ceramic sintered at 650 °C. In addition, τ_f values do not change much with sintering temperature, and fluctuate between -13 and -18 ppm/°C. When the sintering temperature was 650 °C, PZM ceramic possessed the optimal τ_f value of -13.0 ppm/°C.

The concept of chemical bonds in crystals has been widely employed in chemistry and solid physics. And the intrinsic factors affecting the physical properties of crystal could be explored by studying the characteristics of internal chemical bond. P-V-L (Phillps-Van and Vechten-Levine) theory provides methods to calculate the bond properties of binary crystals [42]. According to the research of Zhang et al. complex crystals of PZM could be decomposed to the sum of binary crystals as follows [43]:

$$\begin{aligned} &Pr_2\,Zr_3(MoO_4)_9 \\ &\rightarrow Pr_2 + Zr(1)_1 + Zr(2)_2 + Mo(1)_6 + Mo(2)_3 + O(1)_6 + O(2)_6 + O(3)_6 + O(4)_6 + O(5)_6 + O(6)_6 \\ &\rightarrow Pr_{2/3}O(1)_3 + Pr_{2/3}O(2)_3 + Pr_{2/3}O(6)_3 + Zr(1)O(4)_3 + Zr(2)O(3)_3 + Zr(2)O(5)_3 + Mo(1)_{3/2}O(1)_3 \\ &+Mo(1)_{3/2}O(2)_3 + Mo(1)_{3/2}O(3)_3 + Mo(1)_{3/2}O(4)_3 + Mo(2)_{3/2}O(5)_3 + Mo(2)_{3/2}O(6)_3 \end{aligned} \tag{5}$$

Batsanov et al. found a positive correlation between bond iconicity (*fi*) and dielectric constant as shown in Equation (6) [44]:

$$\varepsilon = \frac{n^2 - 1}{1 - f_i} + 1 \tag{6}$$

where n was the refractive index. The *fi* values can be calculated as Equation (7)-(10). Obviously, the larger iconicity the chemical bond have, the greater the effect on the dielectric constant.

$$f_i^u = (C^u)^2 / (E_g^u)^2 \tag{7}$$

$$(E_g^\mu)^2 = (E_g^\mu)^2 + (C^\mu)^2 \tag{8}$$

$$(E_h^\mu)^2 = \frac{39.74}{(d^\mu)^{2.48}} \tag{9}$$

$$C^\mu = 14.4 b^\mu \exp(-k_s^\mu r_0^\mu)[(Z_A^\mu)^* - \frac{n}{m}(Z_B^\mu)^*] / r_0^\mu \tag{10}$$

where E_μ^h and C^μ were the homopolar part and heteropolar part of μ bond, and E_μ^g was the average energy gap for μ bond. Table 2 listed the calculation results of the ionicity of various chemical bonds in PZM crystal. Since f_i(Pr-O) > f_i(Ti-O) > f_i(Mo-O), it can be think that the ionicity of Pr-O bonds played a decisive role in affecting dielectric constant.

The intrinsic dielectric loss of crystal resulted in the anharmonic terms of lattice vibration. Lattice energy was defined as the released energy during the process by which gaseous ions combine to form solid state. The ionic bonds with higher the lattice energy were more stable, so the lattice energy controlled the stability of the ionic crystal. For a single chemical bond, the lattice energy could be obtained by the following equation:

$$U_{cal} = \sum_{\mu} U_b^{\mu} \tag{11}$$

$$U_{\mathrm{b}}^{\mu} = U_{\mathrm{bc}}^{\mu} + U_{\mathrm{bi}}^{\mu} \tag{12}$$

$$U_{bc}^{\mu} = 2100m\frac{(Z_{+}^{\mu})}{(d^{\mu})^{0.75}} f_c^{\mu} \tag{13}$$

$$U_{bi}^{\mu} = 1270\frac{(m+n)Z_{+}^{\mu}Z_{-}^{\mu}}{d^{\mu}}(1-\frac{0.4}{d^{\mu}}) f_i^{\mu} \tag{14}$$

where Z_{+}^{μ} and Z_{-}^{μ} were the cation valence and anion valence of bond μ, and U_{bc}^{μ} and U_{bi}^{μ} were the covalent part and ionic part of lattice energy, respectively. Moreover, the bond energy of a chemical bond was expressed as the energy required to transform a bonded state into a separate atom, and the more stable the crystal, the higher the energy required to break the bonds. Hence, the bond energy calculated by equation (15)-(19) also has an effect on the quality factor and temperature coefficient of resonance frequency [45,46].

$$E_b^{\mu} = t_c E_c^{\mu} + t_i E_i^{\mu} \tag{15}$$

$$E_c^{\mu} = \frac{(r_{cA} + r_{cB})}{d^{\mu}}(E_{A\text{-}A}E_{B\text{-}B})^{1/2} \tag{16}$$

$$E_i^{\mu} = \frac{1389.088}{d^{\mu}} \tag{17}$$

$$t_c + t_i = 1 \tag{18}$$

$$t_i = \left|\frac{S_A - S_B}{6}\right| \tag{19}$$

where r_{cA} and r_{cB} represented the covalent radius of atom A and atom B, bond energy $E_{A\text{-}A}$ and $E_{B\text{-}B}$ for atom A and atom B can be found in literature [47], t_c and t_i were the covalent coefficient and ion coefficient of chemical bond, and S_A and S_B were the electronegativity of A ion and B ion, respectively. As can be seen from the diagram, Mo-O bond had the highest bond energy and lattice energy among these three different bonds. In result, Mo-O bond played a major role in affecting the stability of the PZM crystal structure, and thus the dielectric loss was also affected by it.

It was well known that the τ_f values were controlled by τ_ε (the temperature coe□cient of permittivity) and α (coe□cient of thermal expansion). On the basis of chemical bonds theory of complex crystals, values of thermal expansion coe□cient could be calculated by the following equation:

$$\tau_f = -\frac{\tau_\varepsilon}{2} - \alpha \tag{20}$$

$$\alpha = \sum_{\mu} F_{mn}^{\mu} \alpha_{mn}^{\mu} \tag{21}$$

where F_{mn}^{μ} was the proportion of muon bonds in the whole chemical bond. For any binary compound, the thermal expansion coefficient can be calculated as follows:

$$\alpha_{mn}^{\mu} = -3.1685 + 0.8376\gamma_{mn} \tag{22}$$

$$r_{mn} = \frac{kZ_A^{\mu} N_{CA}^{\mu}}{U_b^{\mu} \Delta_A} \beta_{mn} \tag{23}$$

$$\beta_{mn} = \frac{m(m+n)}{2n} \tag{24}$$

where k was the Boltzmann constant, Z_A^{μ} was the cation valence state, and N_{CA}^{μ} was the coordination number of cation A. Δ_A was the periodic constant of cation, and that values of the fourth and fifth periods are 1.56 and 1.74, respectively. The average α for Pr-O, Zr-O, and Mo-O were 10.2084×10^{-6}/K, 3.5373×10^{-6}/K, -0.3750×10^{-6}/K, respectively. As a result, Mo-O bond had a positive influence on τ_f values, whereas Pr-O and Zr-O have a negative effect.

In order to further study the intrinsic dielectric properties at microwave frequencies, infrared reflectivity spectrum of PZM ceramic was fitted based on the classical three parameter harmonic oscillator model:

$$\varepsilon^*(\omega) = \varepsilon_\infty + \sum_{j=1}^{n} \frac{\omega_{pj^2}}{\omega_{oj^2} - \omega^2 - j\gamma_j\omega} \tag{25}$$

where $\varepsilon^*(\omega)$ was the complex dielectric function; ε_∞ was the permittivity due to the electronic polarization contribution at high frequencies; γj, ω_{oj} and ω_{pj} were the damping factor, the transverse frequency, and plasma frequency of the j-th Lorenz oscillator, respectively; and n was the number of polar phonons. Fresnel's reflectivity equation gave the relationship between reflectivity and dielectric function:

$$R(\omega) = \left| \frac{1 - \sqrt{\varepsilon^*(\omega)}}{1 + \sqrt{\varepsilon^*(\omega)}} \right|^2 \tag{26}$$

The infrared reflectivity was fitted based on above theory model, and the fitting spectrum and vibration modes were presented in Fig. 8 (a) and Table 3, respectively. There were 21 vibrational modes after fitting and the

ε_∞ was 3.98. Moreover, Fig. 8 (b) presented the real parts (ε') and imaginary parts (ε'') of the complex permittivity. The measured ε' (10.72) was slightly below that of calculated (13.51), which is probably related to the presence of extrinsic defects in the prepared sample [48].

4. Conclusion

In this work, low-firing microwave dielectric ceramics $Pr_2Zr_3(MoO_4)_9$ were investigated. X-ray powder diffraction analysis indicated that $Pr_2Zr_3(MoO_4)_9$ samples belonged to space group R-3c in trigonal system. According to the SEM images, the compact sample could be obtained when sintered at 650 □. $Pr_2Zr_3(MoO_4)_9$ ceramic sintered at 650 □ possessed ε_r of 10.72, high $Q{\cdot}f$ of 64,200 GHz (at 9.6 GHz) and a negative τ_f of -13 ppm/°C. Based on chemical bonds theory of complex crystals, the ε_r and τ_f were primarily influenced by the bond ionicity of Pr-O bond and thermal expansion coefficient of Mo-O bond, respectively. As for quality factor, it was strongly dependent on the lattice energy as well as bond energy of Mo-O bond. Infrared reflectivity spectrum analysis indicated that the dielectric contribution of the microwave region was mainly due to the absorption of phonon oscillations within the infrared region.

Acknowledgements

This work was supported by the National Natural Science Foundation (No. 51972143). The authors are thankful to the help of Professor Zhenxing Yue and postdoctoral Jie Zhang on the measurement of microwave properties in Tsinghua University. The authors are also thankful to the administrators in IR beamline workstation of National Synchrotron Radiation Laboratory (NSRL) for the help in IR measurement.

References

[1] Manan, Z. Ullah, A.S. Ahmad, A. Ullah, D.F. Khan, A. Hussain, M.U. Khan, Phase microstructure evaluation and microwave dielectric properties of (1-x)$Mg_{0.95}Ni_{0.05}Ti_{0.98}Zr_{0.02}O_3$-x$Ca_{0.6}La_{0.8/3}TiO_3$ ceramics, J. Adv. Ceram. 7 (2018) 72-78.

[2] D. Zhou, L.X. Pang, D.W. Wang, C. Li, B.B. Jin, I.M. Reaney, High permittivity and low loss microwave dielectrics suitable for 5G resonators and low temperature co-fired ceramic architecture, J. Mater. Chem. C. 5 (2017) 10094-10098.

[3] C.C. Li, H.C. Xiang, M.Y. Xu, Y. Tang, L. Fang, Li_2AGeO_4 (A= Zn, Mg): Two novel low-permittivity microwave dielectric ceramics with olivine structure. J. Eur .Ceram. Soc. 38 (2018) 1524-1528.

[4] H.H. Guo, D. Zhou, W.F. Liu, L.X. Pang, D.W. Wang, J.Z. Su, Z.M. Qi, Microwave dielectric properties of temperature□stable zircon□type (Bi, Ce)VO_4 solid solution ceramics, J. Am. Ceram. Soc. 103 (2020) 423-431.

[5] Hsing-I Hsiang, Chih-Cheng Chen, Sue-Yu Yang. Microwave dielectric properties of $Ca_{0.7}Nd_{0.2}TiO_3$ ceramic-filled CaO-B_2O_3-SiO_2 glass for LTCC applications. J. Adv. Ceram. 8 (2019) 345-351.

[6] L. Fang, Z.H. Wei, C.X. Su, F. Xiang, H. Zhang, Novel low-firing microwave dielectric ceramics: $BaMV_2O_7$ (M= Mg, Zn), Ceram. Int. 40 (2014) 16835-16839.

[7] J. Li, L. Fang, H. Luo, J. Khaliq, Y. Tang, C.C. Li, Li_4WO_5: A temperature stable low-firing microwave dielectric ceramic with rock salt structure, J. Eur .Ceram. Soc. 36 (2016) 243-246.

[8] X.Q. Song, W. Lei, Y.Y. Zhou, T. Chen, S.W. Ta, Z.X. Fu, W.Z. Lu, Ultra□low fired fluoride composite microwave dielectric ceramics and their application for $BaCuSi_2O_6$□based LTCC, J. Am. Ceram. Soc. https://doi.org/10.1111/jace.16795.

[9] H.C. Xiang, C.C. Li, H. Jantunen, L. Fang, A.E. Hill, Ultralow Loss $CaMgGeO_4$ microwave dielectric ceramic and its chemical compatibility with silver electrodes for low-temperature cofired ceramic applications, ACS Sustain. Chem. Eng. 6 (2018) 6458-6466

[10] X.K. Lan, J. Li, Z.Y. Zou, G.F. Fan, W.Z. Lu, W. Lei, Lattice structure analysis and optimised microwave dielectric properties of $LiAl_{1-x}(Zn_{0.5}Si_{0.5})_xO_2$ solid solutions, J. Eur. Ceram. Soc. 39 (2019) 2360-2364.

[11] K. Du, X.Q. Song, J. Li, J. Wu, W.Z. Lu, X.C. Wang, W. Lei, Optimised phase compositions and improved microwave dielectric properties based on calcium tin silicates, J. Eur. Ceram. Soc. 39 (2019) 340-345.

[12] L.X. Pang, D. Zhou, Modification of $NdNbO_4$ microwave dielectric ceramic by Bi substitutions, J. Am. Ceram. Soc. 102 (2019) 2278-2282.

[13] W.J. Guo, J. Zhang, Y. Luo, Z.X. Yue, L.T. Li, Microwave dielectric properties and thermally stimulated depolarization of Al-doped $Ba_4(Sm, Nd)_{9.33}Ti_{18}O_{54}$ ceramics, J. Am. Ceram. Soc., 102 (2019) 5494-5502.

[14] W. Lei, Z.Y. Zou, Z.H. Chen, B Ullah, A. Zeb, X.K. Lan, W.Z. Lu, G.F. Fan, X.H. Wang, X.C. Wang, Controllable τ_f value of barium silicate microwave dielectric ceramics with different Ba/Si ratios, J. Am. Ceram. Soc. 101 (2018) 25-30.

[15] M. Wu, Y.C. Zhang, M.Q. Xiang. Synthesis, characterization and dielectric properties of a novel temperature stable (1-x)$CoTiNb_2O_8$-x$ZnNb_2O_6$ ceramic. J. Adv. Ceram. 8 (2019) 228-237.

[16] D. Zhou, L.X. Pang, D.W. Wang, L.M. Reaney, Novel water-assisting low firing MoO_3 microwave dielectric ceramics, J. Eur. Ceram. Soc. 39 (2019) 2374-2378.

[17] H.Y. Yang, S.R. Zhang, Y.W. Chen, H.C. Yang, Y. Yuan, E.Z. Li, Crystal chemistry, Raman spectra, and bond characteristics of trirutile-type $Co_{0.5}Ti_{0.5}TaO_4$ microwave dielectric ceramics, Inorg. Chem. 58 (2019) 968-976.

[18] J.X. Bi, CF Xing, C.H. Yang, H.T. Wu, Phase composition, microstructure and microwave dielectric properties of rock salt structured Li_2ZrO_3-MgO ceramics, J. Eur. Ceram. Soc. 38 (2018) 40-46.

[19] L. Fang, C.X. Su, H.F. Zhou, Z.H. Wei, H. Zhang Novel low□firing microwave dielectric ceramic $LiCa_3MgV_3O_{12}$ with low dielectric loss, J. Am. Ceram. Soc. 96 (2013) 688-690.

[20] H.C. Xiang, L. Fang, W.S. Fang, Y. Tang, C.C. Li, A novel low-firing microwave dielectric ceramic $Li_2ZnGe_3O_8$ with cubic spinel structure, J. Eur .Ceram. Soc. 37 (2017) 625-629.

[21] C.X. Su, L. Fang, Z.H. Wei, X.J. Kuang, H. Zhang, $LiCa_3ZnV_3O_{12}$: A novel low-firing, high Q microwave dielectric ceramic, Ceram. Int. 40 (2014) 5015-5018.

[22] A. Maqbool, A. Hussain, J.U. Rahman, T.K. Song, W.J. Kim, J. Lee, M.H. Kim, Enhanced electric field-induced strain and ferroelectric behavior of $(Bi_{0.5}Na_{0.5})TiO_3$-$BaTiO_3$-$SrZrO_3$ lead-free ceramics, Ceram. Int. 40 (2014) 11905-11914.

[23] S. Kim, H. Choi, S. Han, J.S. Park, M.H. Lee, T.K. Song, M.H. Kim, D. Doc, W.J. Kim, A correlation between piezoelectric response and crystallographic structural parameter observed in lead-free (1-x)$(Bi_{0.5}Na_{0.5})TiO_3$-x$SrTiO_3$ piezoelectrics, J. Eur. Ceram. Soc. 37 (2017) 1379-1386.

[24] A. Maqbool, A. Hussain, J.U. Rahman, J.K. Park, T.G. Park, J.S. Song, M.H. Kim, Effect of $SrZrO_3$ substitution on structural and electrical properties of lead-free $Bi_{0.5}Na_{0.5}TiO_3$-$BaTiO_3$ ceramics, Phys. Status. Solidi. A 211 (2014) 1709-1714.

[25] R. Hatel, S.E. Majdoub, A. Bakour, M. Khenfouch, M. Baitoul, Graphene oxide/Fe_3O_4 nanorods composite: structural and Raman investigation, J. Phys. Conf. Series. 1081 (2018) 012006.

[26] X.L. Chen, X. Li, H.F. Zhou, J. Sun, X.X. Li, X. Yan, C.C. Sun, J.P. Shi. Phase evolution, microstructure, electric properties of $(Ba_{1-x}Bi_{0.67x}Na_{0.33x})(Ti_{1-x}Bi_{0.33x}Sn_{0.67x})O_3$ ceramics. J. Adv. Ceram. 8 (2019) 427-437.

[27] S.Z. Hao, D. Zhou, L.X. Pang, The spectra analysis and microwave dielectric properties of $[Ca_{0.55}(Sm_{1-x}Bi_x)_{0.3}]MoO_4$ ceramics, J. Am. Ceram. Soc. 102 (2019) 3103-3109.

[28] H.H. Guo, D. Zhou, L.X. Pang, Z.M. Qi, Microwave dielectric properties of low firing temperature stable scheelite structured (Ca, Bi)(Mo, V)O_4 solid solution ceramics for LTCC applications, J. Eur. Ceram. Soc. 39 (2019) 2365-2373.

[29] S.G. Dorzhieva, Y.L. Tushinova, B.G. Bazarov, A.I. Nepomniashchikh, R.Y. Shendrik, Z.G. Bazarova, Luminescence of Ln-Zr molybdates, Bull. Russ. Acad. Sci.: Phys. 79 (2015) 276-279.

[30] J.G. Bazarova, Y.L. Tushinova, B.G. Bazarov, S.G. Dorzhieva, Double molybdates of rare earth elements and zirconium, Russ. Chem. Bull. 66 (2017) 587-592.

[31] W.Q. Liu, R.Z. Zuo, A novel low-temperature firable $La_2Zr_3(MoO_4)_9$ microwave dielectric ceramic, J. Eur. Ceram. Soc. 38 (2018) 339-342.

[32] H. Zhang, H.T. Wu, Crystal structure and microwave dielectric properties of $La_2(Zr_{1-x}Ti_x)_3(MoO_4)_9$ ($0 \leq x \leq 0.1$) ceramics, J. Am. Ceram. Soc. 102 (2019) 4092-4102.

[33] W.Q. Liu, R.Z. Zuo, Low temperature fired $Ln_2Zr_3(MoO_4)_9$ (Ln = Sm, Nd) microwave dielectric ceramics, Ceram. Int. 43 (2017) 17229-17232.

[34] Y.H. Zhang, J.J. Sun, N. Dai, Z.C. Wu, H.T. Wu, C.H. Yang, Crystal structure, infrared spectra and microwave dielectric properties of novel extra low-temperature fired $Eu_2Zr_3(MoO_4)_9$ ceramics, J. Eur. Ceram. Soc. 39 (2019) 1127-1131.

[35] C.F. Xing, B. Wu, J. Bao, H.T. Wu, Y.Y. Zhou, Crystal structure, infrared spectra and microwave dielectric properties of a novel low-firing $Gd_2Zr_3(MoO_4)_9$ ceramic, Ceram. Int. 45 (2019) 22207-22214.

[36] B.W. Hakki, P.D. Coleman, A dielectric resonator method of measuring inductive capacities in the millimeter range, IRE Trans. Microw. Theory Tech. 8 (1960) 402-410.

[37] W.E. Courtney, Analysis and evaluation of a method of measuring the complex permittivity and permeability microwave insulators, IEEE Trans. Microw. Theory Tech. (18) 1970 476-485.

[38] R.F. Klevtsova, S.F. Solodovnikov, Y.L. Tushinova, B.G. Bazarov, L.A. Glinskaya, Z.G. Bazarova, A new type of mixed framework in the crystal structure of binary molybdate $Nd_2Zr_3(MoO_4)_9$, J. Struc. Chem. 41 (2000) 280-284.

[39] A.J. Bosman, E.E. Havinga, Temperature dependence of dielectric constants of cubic ionic compounds, Phys. Rev. 129 (1963) 1593-1600.

[40] R.D. Shannon, Dielectric polarizabilities of ions in oxides and fluorides, J. Appl. Phys. 73 (1993) 348-366.

[41] G.K. Choi, JR Kim, SH Yoon, KS Hong, Microwave dielectric properties of scheelite (A = Ca, Sr, Ba) and wolframite (A = Mg, Zn, Mn) $AMoO_4$ compounds, J. Eur. Ceram. Soc. 27 (2007) 3063-3067.

[42] B.F. Levine, Bond susceptibilities and ionicities in complex crystal structures, J. Chem. Phys. 59 (1973) 1463-1486.

[43] S.Y. Zhang, The study of chemical bonds theory of complex crystals. Chinese J. Chem. Phys. 4 (1991) 109-115.

[44] S.S. Batsanov, Dielectric methods of studying the chemical bond and the concept of electronegativity, Russ. Chem. Rev. 51 (1982) 684-697.

[45] R.T. Sanderson, Multiple and single bond energies in inorganic molecules, Inorg. Nucl. Chem. 30 (1968) 375-393.

[46] R.T. Sanderson, Electronegativity and bond energy, J. Am. Chem. Soc. 105 (1983) 2259-2261.

[47] Y.R. Luo, Comprehensive handbook of chemical bond energies, Boca Raton, FL: CRC Press; 2007.

[48] J. Petzelt, S. Kamba, Submillimetre and infrared response of microwave materials: extrapolation to microwave properties, Asia. Pacific. Microwave. Conference. 79 (2003) 175-180.

Figure captions

Fig. 1 (a) XRD patterns and (b) Rietveld refinement of $Pr_2Zr_3(MoO_4)_9$ ceramics sintered at 650 □.

Fig. 2 Schematic diagram of crystal structure for $Pr_2Zr_3(MoO_4)_9$.

Fig. 3 Apparent and relative density for $Pr_2Zr_3(MoO_4)_9$ ceramics sintered at different temperatures.

Fig. 4 SEM images of $Pr_2Zr_3(MoO_4)_9$ ceramics sintered 600 □ (a), 650 □ (b), 700 □ (c), 750 □ (d), 800 □.

Fig. 5 The variation of ε_r values for $Pr_2Zr_3(MoO_4)_9$ ceramics as a function of sintering temperature.

Fig. 6 $Q•f$ and τ_f values of $Pr_2Zr_3(MoO_4)_9$ ceramics as a function of sintering temperature.

Fig. 7 Bar diagram of chemical bond parameter ((a)iconicity, (b) bond energy, (c)lattice energy, and (d) thermal expansion coefficient) in $Pr_2Zr_3(MoO_4)_9$ compounds.

Fig. 8 (a) Measured and calculated infrared reflectance spectrum, and (b) real and imaginary parts of the complex permittivity for $Pr_2Zr_3(MoO_4)_9$ compounds sintered at 650 □.

Table captions

Table 1 Refined lattice parameters and reliability factors for $Pr_2Zr_3(MoO_4)_9$ ceramics sintered at various temperature.

Table 2 Chemical bond parameter (iconicity, bond energy, lattice energy, and thermal expansion coefficient) of $Pr_2Zr_3(MoO_4)_9$ ceramics sintered at 650 □.

Table 3 Phonon parameters calculated from the fitting of the infrared reflectance spectrum of $Pr_2Zr_3(MoO_4)_9$.

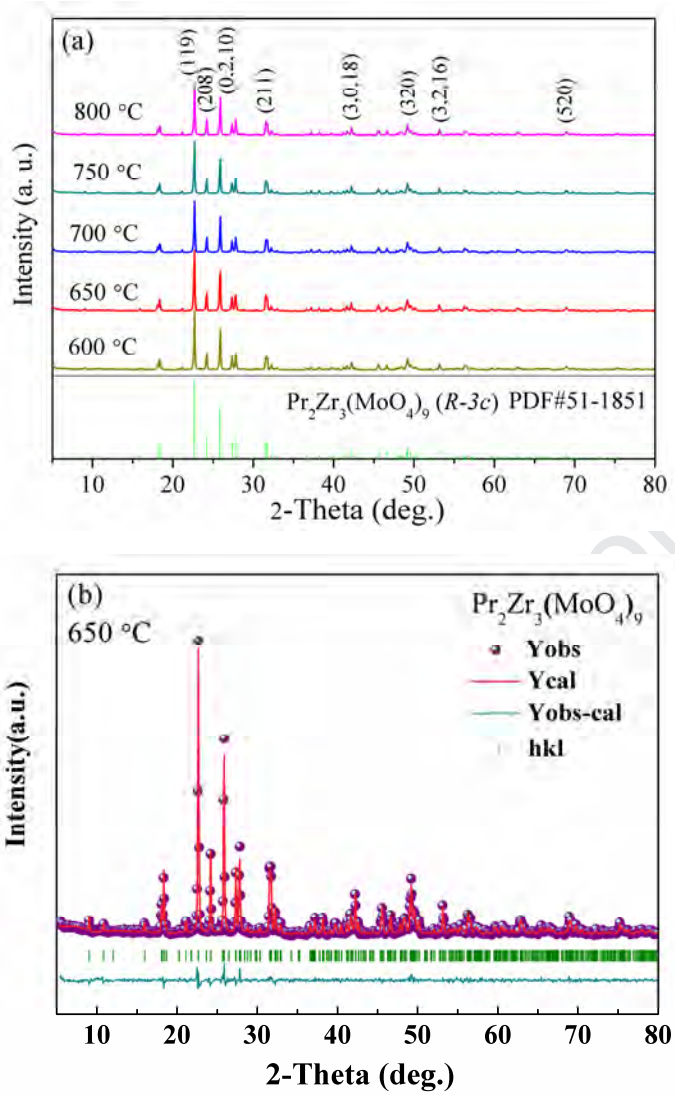
(a)
(119)
(208)
(0,2,10)
(211)
(3,0,18)
(320)
(3,2,16)
(520)
800 °C
750 °C
700 °C
650 °C
600 °C
Pr2Zr3(MoO4)9 (R-3c) PDF#51-1851
Intensity (a. u.)
10
20
30
40
50
60
70
80
2-Theta (deg.)
(b)
650 °C
Pr2Zr3(MoO4)9
Yobs
Ycal
Yobs-cal
hkl
Intensity(a.u.)
10
20
30
40
50
60
70
80
2-Theta (deg.)

Fig.1

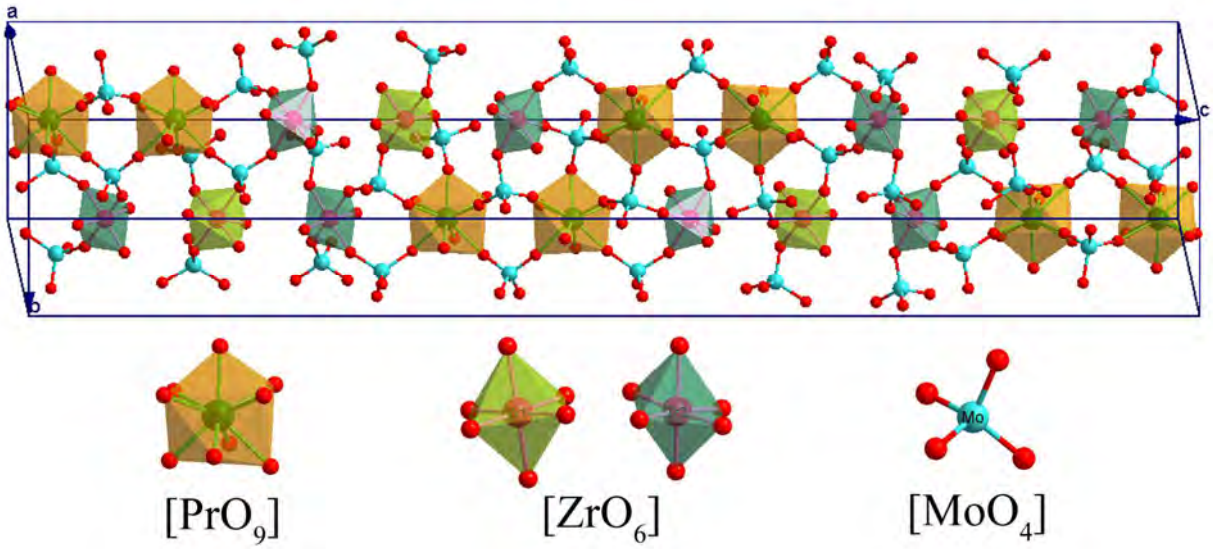

Fig.2

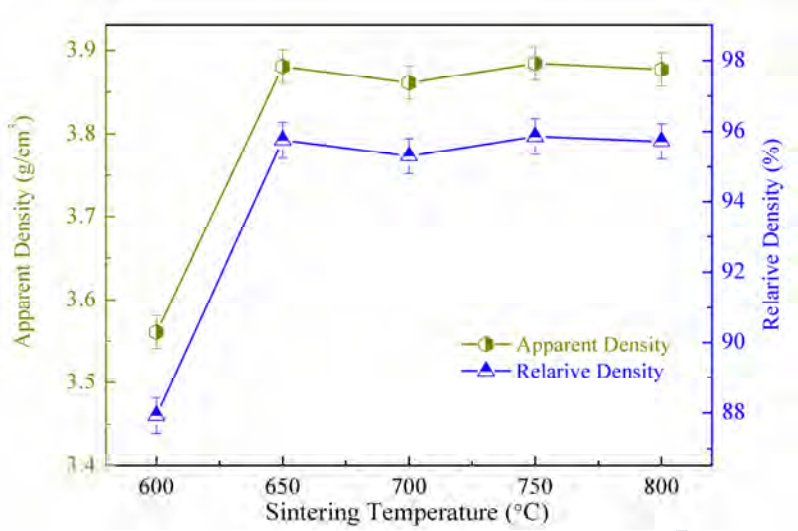

Fig.3

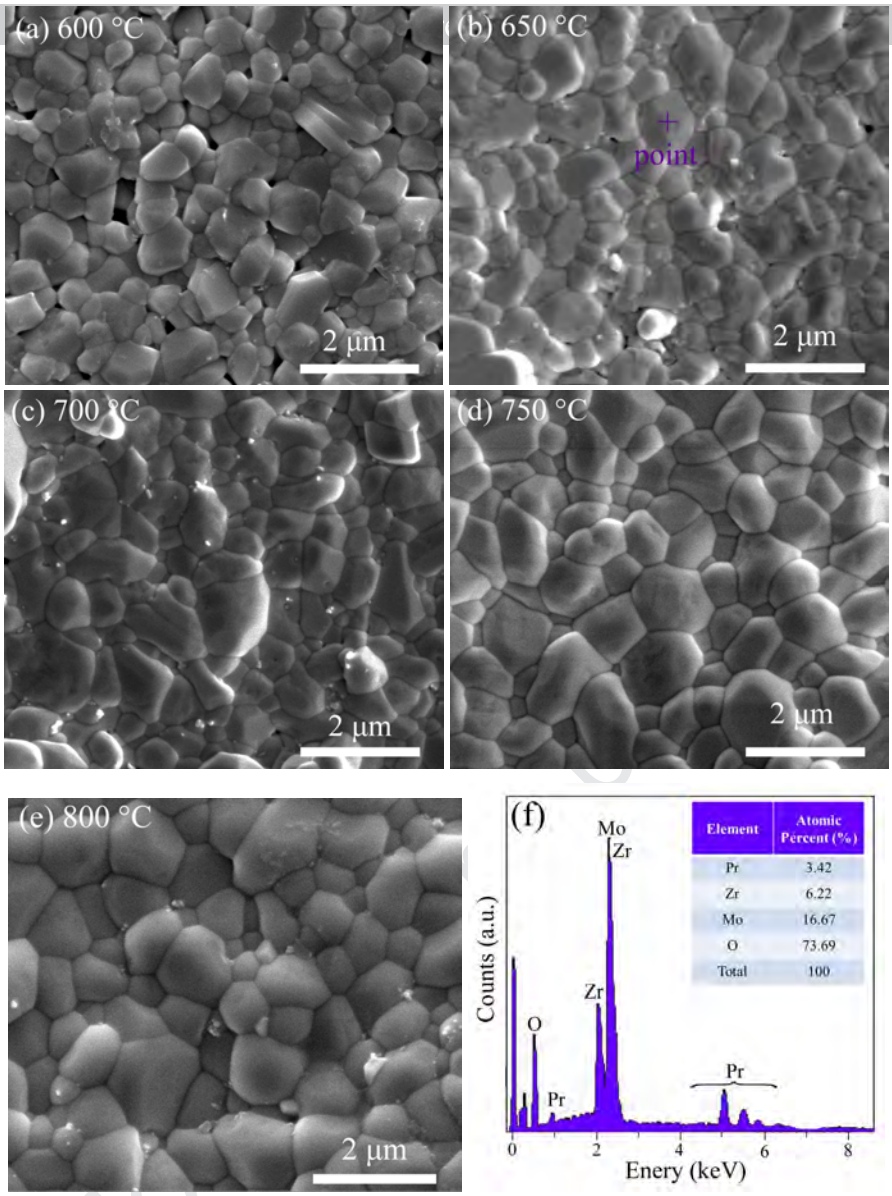
(a) 600 °C
2 μm
(b) 650 °C
point
2 μm
(c) 700 °C
2 μm
(d) 750 °C
2 μm
(e) 800 °C
2 μm
(f)
Mo
Zr
Zr
O
Pr
Pr
Counts (a.u.)
0
2
4
6
8
Enery (keV)
Element
Atomic Percent (%)
Pr 3.42
Zr 6.22
Mo 16.67
O 73.69
Total 100

Fig.4

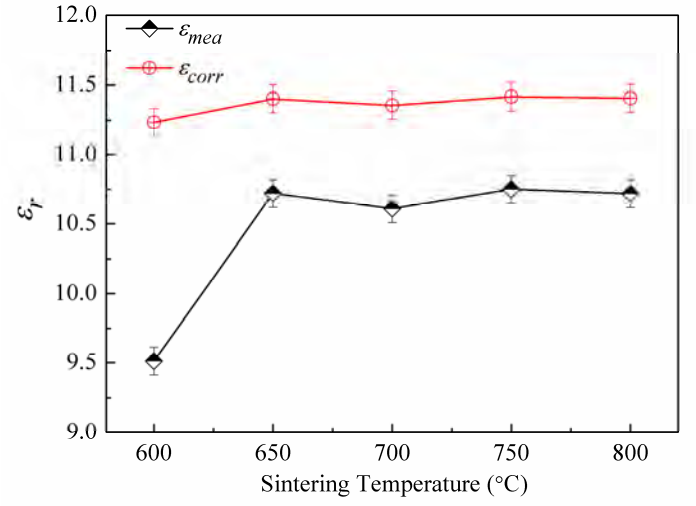

Fig.5

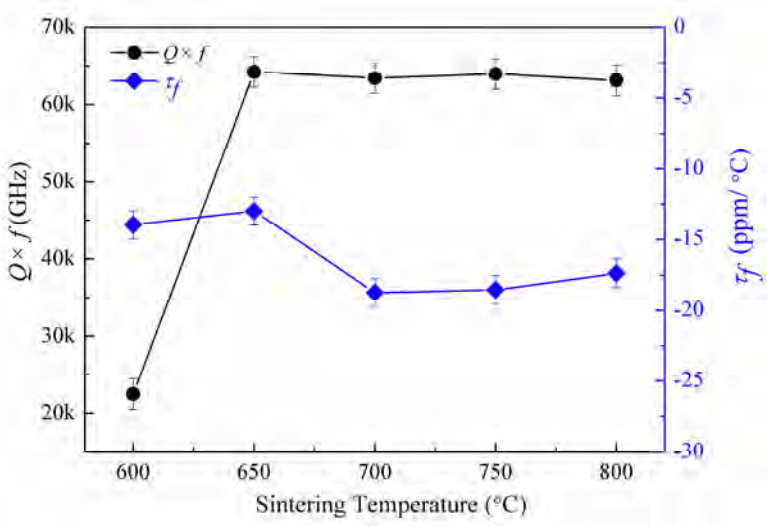

Fig.6

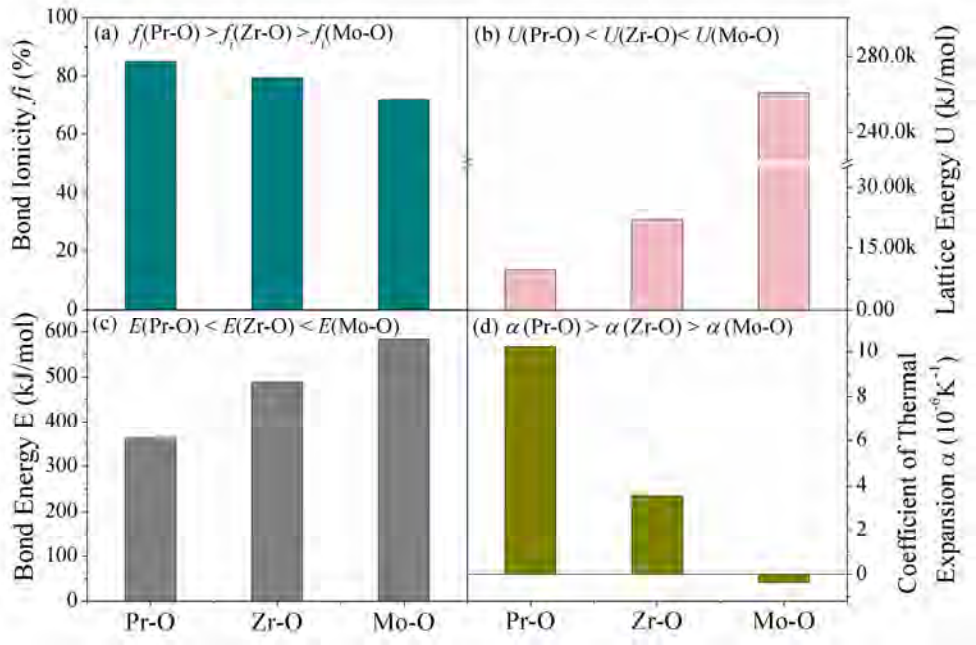

Fig.7

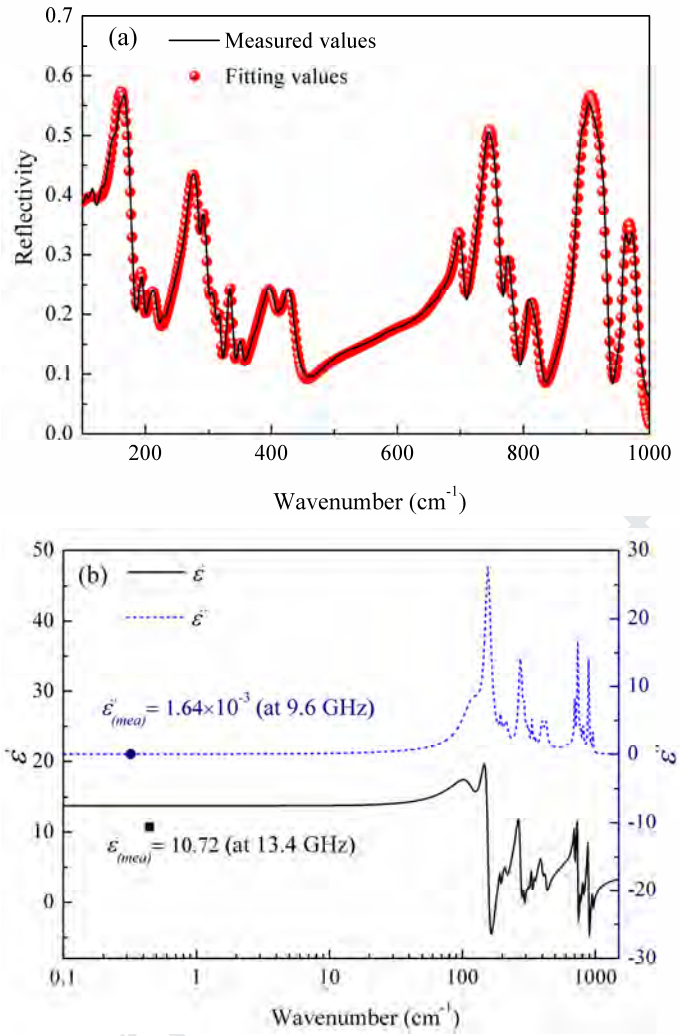
(a)
Measured values
Fitting values
Reflectivity
Wavenumber (cm-1)
(b)
ε'
ε''
ε''(mea) = 1.64×10-3 (at 9.6 GHz)
ε'(mea) = 10.72 (at 13.4 GHz)
Wavenumber (cm-1)

Fig.8

Table 1

S.T. (°C)	$a=b$ (Å)	c (Å)	V_{unit} (Å^3)	R_p (%)	R_{wp} (%)	χ^2
600	9.823(1)	58.729(2)	4907.7(0)	6.78	8.80	1.55
650	9.821(0)	58.716(8)	4904.5(7)	7.10	9.06	1.79
700	9.820(4)	58.739(7)	4905.9(1)	7.67	9.91	2.05
750	9.820(9)	58.732(8)	4905.8(2)	6.77	8.77	1.30
800	9.821(0)	58.749(4)	4907.3(2)	7.13	9.20	1.58

Table 2

Bond type	*d* (Å)	f_i^{μ}	U_{bc} (kJ/mol)	U_{bi} (kJ/mol)	U (kJ/mol)	E_i (kJ/mol)	E_c (kJ/mol)	E (kJ/mol)	α ($10^{-6}K^{-1}$)
Pr-O(1)[1]	2.493(2)	0.850(1)	211	877	1088	243.150(7)	556.884(3)	363.938(1)	10.133(6)
Pr -O(1)[2]	2.493(7)	0.850(1)	211	877	1088	243.101(9)	556.772(7)	363.865(2)	10.133(6)
Pr -O(1)[3]	2.494(1)	0.850(1)	211	877	1088	243.062(9)	556.683(4)	363.806(8)	10.137(7)
Pr -O(2)[1]	2.439(2)	0.850(6)	210	875	1085	248.533(6)	569.212(9)	371.995(1)	9.888(8)
Pr -O(2)[2]	2.439(5)	0.850(6)	210	874	1084	248.503(1)	569.142(9)	371.949(4)	9.888(8)
Pr -O(2)[3]	2.439(9)	0.850(6)	210	874	1084	248.462(4)	569.049(6)	371.888(4)	9.892(7)
Pr -O(6)[1]	2.596(9)	0.851(8)	206	869	1075	233.441(1)	534.646(7)	349.405(3)	10.599(9)
Pr -O(6)[2]	2.597(2)	0.851(8)	206	869	1075	233.414(2)	534.584(9)	349.364(9)	10.599(9)
Pr -O(6)[3]	2.597(6)	0.851(9)	206	869	1075	233.378(2)	534.502(6)	349.311(1)	10.599(9)
Zr(1)-O(4)×6	2.022(7)	0.791(6)	2413	8187	10600	413.574(4)	686.421(1)	509.525(5)	3.307(2)
Zr(2)-O(3)[1]	2.213(8)	0.779(7)	896	2834	3730	377.873(8)	627.167(8)	465.542(2)	3.781(4)
Zr(2)-O(3)[2]	2.214(4)	0.779(8)	896	2834	3730	377.771(4)	626.997(8)	465.41(6)	3.782(8)
Zr(2)-O(3)[3]	2.214(6)	0.7798	895	2834	3729	377.737(3)	626.941(2)	465.37(4)	3.783(4)
Zr(2)-O(5)[1]	2.047(1)	0.7894	821	2750	3571	408.644(9)	678.239(5)	503.452(3)	3.367(7)
Zr(2)-O(5)[2]	2.047(3)	0.7895	821	2749	3570	408.605(0)	678.173(2)	503.403(1)	3.368(3)
Zr(2)-O(5)[3]	2.047(9)	0.7895	821	2749	3570	408.485(3)	677.974(5)	503.255(7)	3.370(1)
Mo(1)-O(1)	1.689(0)	0.7074	12028	33590	45618	554.411(3)	822.039(1)	611.505(2)	-0.473(6)
Mo(1)-O(2)	1.828(6)	0.7120	11627	33269	44896	512.086(1)	759.282(5)	564.821(4)	-0.321(7)
Mo(1)-O(3)	1.713(0)	0.7275	10316	32007	42323	546.643(7)	810.521(9)	602.937(7)	-0.447(6)
Mo(1)-O(4)	1.929(5)	0.7341	9774	31375	41149	485.307(4)	719.577(1)	535.285(0)	-0.210(9)
Mo(2)-O(5)×2	1.892(3)	0.709(8)	11817	33424	45241	494.847(9)	733.723(0)	545.807(9)	-0.251(8)
Mo(2)-O(6)×2	1.623(1)	0.731(9)	9952	31590	41542	576.921(1)	855.414(9)	636.333(1)	-0.544(7)
Pr-$O_{avg.}$	2.510(1)	0.850(9)	-	-	-	-	-	361.724(9)	10.208(4)
Zr-$O_{avg.}$	2.115(4)	0.785(6)	-	-	-	-	-	487.995(5)	3.537(3)
Mo-$O_{avg.}$	1.779(3)	0.720(4)	-	-	-	-	-	582.781(7)	-0.375(0)

Table 3

Mode	ω_{oj}	ω_{pj}	γ_j	$\Delta\varepsilon_j$
1	121.08	201.24	51.723	3.11
2	156.32	279.05	19.828	1.51
3	193.89	59.152	6.5796	1.53
4	213.17	119.09	20.951	0.12
5	273.74	275.51	21.101	0.25
6	291.66	98.78	9.3837	0.03
7	306.74	98.701	14.473	0.94
8	316.81	55.029	6.339	0.14
9	334.34	106.74	8.9373	0.10
10	351.48	72.755	10.858	0.03
11	397.57	200.12	27.303	0.10
12	426.62	202.01	26.727	0.04
13	520.1	280.68	221.66	0.20
14	620.71	200.69	93.891	0.29
15	677.82	165.71	36.718	0.10
16	699.2	237.24	12.434	0.48
17	739.58	496.05	20.547	0.07
18	774.63	186.61	15.45	0.09
19	811.57	262.14	25.172	0.35
20	891.18	506.61	20.753	0.01
21	957.56	216.66	17.342	0.04
$Pr_2Zr_3(MoO_4)_9$	ε_∞=3.98		ε_0=13.51	

Research highlights

- A novel $Pr_2Zr_3(MoO_4)_9$ microwave dielectric ceramic was prepared.
- Rietveld refinement was used to obtain the lattice parameters.
- Relationships among intrinsic factors, phonons and dielectric properties were investigated.
- Optimum dielectric properties were obtained in $Pr_2Zr_3(MoO_4)_9$ ceramic sintered at low temperature of 650 °C.

Declaration of interests

☐ The authors declare that they have no known competing financial interests or personal relationships that could have appeared to influence the work reported in this paper.

☒ The authors declare the following financial interests/personal relationships which may be considered as potential competing interests: